

Bayesian Heuristics for Robust Spatial Perception

Aamir Hussain Chughtai, Muhammad Tahir and Momin Uppal

Abstract—Spatial perception is a key task in several machine intelligence applications such as robotics and computer vision. In general, it involves the nonlinear estimation of hidden variables that represent the system’s state. However, in the presence of measurement outliers, the standard nonlinear least squared formulation results in poor estimates. Several methods have been considered in the literature to improve the reliability of the estimation process. Most methods are based on heuristics since guaranteed global robust estimation is not generally practical due to high computational costs. Recently general purpose robust estimation heuristics have been proposed that leverage existing non-minimal solvers available for the outlier-free formulations without the need for an initial guess. In this work, we propose three Bayesian heuristics that have similar structures. We evaluate these heuristics in practical scenarios to demonstrate their merits in different applications including 3D point cloud registration, mesh registration and pose graph optimization. The general computational advantages our proposals offer make them attractive candidates for spatial perception tasks.

Index Terms—Spatial Perception, Measurement Outliers, Non-linear Estimation, Variational Bayes, Expectation-Maximization, Statistical Inference, Parameter and State Estimation.

I. INTRODUCTION

Several machine intelligence tasks in robotics depend on reliable spatial perception which involves the estimation of the unknown latent variable representing the state describing the system. Examples of spatial perception include object detection and localization, motion estimation, simultaneous localization and mapping (SLAM) [1]–[4] etc. The information for inference is available in form of noisy observations which can generally be represented as transformations of the hidden variable given as

$$\mathbf{y}_i = \mathbf{h}_i(\mathbf{x}) + \epsilon_i \quad (1)$$

where the i th measurement \mathbf{y}_i ($i = 1, \dots, m$), of a batch of data \mathbf{y} , is expressed as a known nonlinear function $\mathbf{h}_i(\cdot)$ of the unknown variable of interest \mathbf{x} corrupted by random noise ϵ_i . Under the assumption that ϵ_i , described with zero-mean Gaussian noise statistics with the precision matrix Ω_i (inverse of the covariance matrix), is uncorrelated across each measurement channel, the *maximum a posteriori* (MAP) estimate has the following equivalent least square formulation [3]

$$\operatorname{argmin}_{\mathbf{x} \in \mathcal{X}} \sum_{i=0}^m \|\mathbf{y}_i - \mathbf{h}_i(\mathbf{x})\|_{\Omega_i}^2 = \operatorname{argmin}_{\mathbf{x} \in \mathcal{X}} \sum_{i=0}^m (r_i(\mathbf{y}_i, \mathbf{x}))^2 \quad (2)$$

where \mathcal{X} denotes the domain of \mathbf{x} , the notation $\|e\|_{\Omega}^2 = \mathbf{e}^\top \Omega \mathbf{e}$ and $r_i(\mathbf{y}_i, \mathbf{x})$ is the residual error for the i th measurement.

The authors are with Department of Electrical Engineering, Lahore University of Management Sciences, DHA Lahore Cantt., 54792, Lahore Pakistan. (email: chughtaiah@gmail.com; tahir@lums.edu.pk; momin.uppal@lums.edu.pk)

Note that $r_0(\mathbf{y}_0, \mathbf{x})$ incorporates the regularizing term considering a Gaussian prior for \mathbf{x} . It is well known that the cost function in (2) leads to brittle estimates in face of measurement outliers owing to unwanted over-fitting to the corrupted data [5]. The observations can be easily plagued with outliers in practice due to sensor failures, environmental factors, or due to erroneous data association by the preprocessing front-end algorithms [6], [7]. This limits the reliability of perception-based tasks and is therefore a dynamic research area in robotics.

Owing to the underlying functional nonlinearities and non-convexity of the domain, even solving (2) globally for common spatial perception applications can be challenging. However, several estimators have been devised in this regard for various applications including point cloud registration, mesh registration, pose graph optimization [8]–[10] etc. These are commonly termed as *non-minimal* solvers which utilize all the measurements for estimation. On the other hand, *minimal* solvers use the smallest number of observations for estimation [11].

The problem of estimation in the presence of outliers becomes more complicated since the standard cost function in (2) is inadequate for this purpose. Therefore, several approaches have been devised in this regard. Most of the methods are heuristics that offer efficient solutions mostly without guarantees [11]–[15]. Other specialized guaranteed approaches also exist that provide solutions with formal certificates. However, their practicality gets limited due to issues with scalability to large-scale problems as the underlying semidefinite programs (SDP) can have a very high computational budget [16], [17]. Naturally, efficient heuristics become the default choice to enable such applications. In the literature, hybrid approaches have also been advocated where the solutions obtained from heuristics are subsequently evaluated for optimality [18]. Since these hybrid approaches have been found to work effectively in practice, efficient heuristics are highly desired.

Different general purpose heuristics for robust spatial perception have been designed based on consensus maximization aiming to maximize observations within a predefined inlier threshold during estimation [6]. The famous random sample consensus (RANSAC) approach [12] is extensively employed relying on minimal solvers for operation. Realizing the fragility of RANSAC under a high outlier regime and its scalability issues, Adaptive Trimming (APAPT) has been proposed to address these limitations [13]. ADAPT adopts non-minimal solvers in its design.

Another popular approach is M-estimation [19] which relies on robust cost functions applied to the residuals for resilience against data corruption. Since these formulations are generally inefficient to solve globally [6], the recently introduced graduated non-convexity (GNC) approach proposes an efficient

heuristic [11]. It replaces the underlying non-convex functions with surrogate functions for two common cost functions namely the Geman McClure (GM) and the truncated least square (TLS). Using the Black-Rangarajan duality it casts an equivalent formulation which is then iteratively solved using variable and weight update steps alternatively resulting in GNC-GM and GNC-TLS methods. These are general-purpose robust estimators that employ non-minimal solvers during the variable update step and require no initial guess for operation.

The relevant literature also indicates the use of Bayesian methods for outlier-robust estimation. In [20], a method to tune M-estimators is suggested. It aims to estimate the tuning parameters of the M-estimators within an Expectation Maximization (EM) framework. However, the overall scheme is complicated due to its reliance on adaptive importance sampling. Another Bayesian EM-based method is reported in [15] where the parameters of a general robust function are estimated along with the primary variable of interest. The method invokes iteratively reweighted least squares (IRLS) within its EM framework which adds an additional layer of approximation during inference since IRLS performance can be sensitive to initialization. Other Bayesian methods, reported in the filtering context, do not involve M-estimation for inference. For example, methods in [21], [22] propose handling outliers by modifying the standard Gaussian likelihood distributions and subsequently perform inference. However, these algorithms do not treat outliers independently for each measurement channel due to under-parameterization [23]. Obviating this limitation, two similar Bayesian methods have been proposed: the recursive outlier-robust (ROR) [24] and the selective observations rejecting (SOR) [23] method. We build on these two methods for the general nonlinear robust estimation problem with the following contributions.

- We study the limitations of the standard ROR and SOR methods which shows why these standard approaches falter in spatial perception applications. The analysis suggests the need for adapting the hyper-parameters, governing the outlier characteristics, during inference.
- We propose three methodologies to overcome the shortcomings of the standard approaches. Similar to the GNC methods, we are interested in invoking the existing non-minimal estimators. To this end, we consider point estimates for \mathbf{x} and use the EM framework. Since EM can be viewed as a special case of variational Bayes (VB), the adaptation is possible. The proposed approaches are similar to the iterative GNC methods with alternating variable and weight update steps.
- We also evaluate the proposals in several experimental scenarios and benchmark them against the GNC methods which are the state-of-the-art general purpose heuristics for robust spatial perception.

The structure of the remaining paper is as follows. In Section II, we motivate the selection of the ROR and SOR methods which we build upon. Moreover, we discuss the inferential tools employed in our proposals. In Section III, we discuss the limitations of the standard approaches and present methodologies to overcome their shortcomings. In Section IV,

we discuss the experimental results. Lastly, Section V provides concluding remarks along with some future directions.

II. RELEVANT BAYESIAN METHODS AND TOOLS

In this section, we first briefly discuss the motivation for choosing the two Bayesian methods: ROR and SOR. Moreover, we provide a short primer on the Bayesian tools that we leverage in our proposals in the upcoming section.

A. Choice of the Bayesian methods for robust estimation

Recently, ROR and SOR methods have been successfully applied for devising robust nonlinear filtering techniques with satisfactory performance results. In these methods, estimation of \mathbf{x} in (1) relies on modifying the measurement noise statistics. The choice is motivated by the inability of the nominal Gaussian noise to describe the data in face of outliers. Subsequently, the noise parameters are jointly estimated with \mathbf{x} . Bayesian theory offers attractive inferential tools for estimating the state and parameters jointly enabling iterative solutions [25], [26]. We adapt these methods to the general nonlinear estimation context of (1) and (2) where non-minimal solvers for estimation are available for the outlier-free cases. The motivation for choosing these particular methods is twofold. First, the formulations of these filters lend their modification conveniently to the nonlinear problem at hand. Moreover, owing to the modeling simplicity, the choice of the hyperparameters for the noise statistics is intuitive for adaptation to our case.

B. EM as a special case of VB

For solving the problem in (2), we aim to use non-minimal solvers, which have been developed and tested for different applications. To that end, we need to cast the ROR and SOR algorithms in a way that existing nonlinear least squared solvers are invoked during inference. These Bayesian methods are devised using VB which leads to distributions for the state and parameters. However, the available solvers generally result in point estimates for the state. Therefore, to enable adoption of these Bayesian approaches for robust spatial perception applications, we adopt the EM method which as shown in the Bayesian literature can be viewed as a special case of the VB algorithm [27]. We first present the VB method and then interpret EM method as its special case.

1) *VB*: Suppose that we are interested in estimating multivariate parameter $\boldsymbol{\theta}$ from data \mathbf{y} . For tractability, we can resort to the VB algorithm considering the mean-field approximation where the actual posterior is approximated with a factored distribution as [28]

$$p(\boldsymbol{\theta}|\mathbf{y}) \approx \prod_{j=1}^J q(\boldsymbol{\theta}_j) \quad (3)$$

where J partitions of $\boldsymbol{\theta}$ are assumed with the j th partition given as $\boldsymbol{\theta}_j$. The VB marginals can be obtained by minimizing the Kullback-Leibler (KL) divergence between the product approximation and the true posterior resulting in

$$q(\boldsymbol{\theta}_j) \propto e^{\langle \ln(p(\boldsymbol{\theta}|\mathbf{y})) \rangle_{q(\boldsymbol{\theta}_j)}} \quad \forall j \quad (4)$$

where $q(\boldsymbol{\theta}_{-j}) = \prod_{k \neq j} q(\boldsymbol{\theta}_k)$ and $\langle \cdot \rangle_{q(\mathbf{x})}$ denotes the expectation of the argument with respect to the distribution $q(\mathbf{x})$. The VB marginals can be obtained by iteratively invoking (4) till convergence.

2) *EM*: From the Bayesian literature, we know that the EM method can be viewed as a special case of the VB algorithm considering point densities for some of the factored distributions in (3). In particular, the factored distributions which are assumed as point masses in (3) can be written as delta functions

$$q(\boldsymbol{\theta}_n) = \delta(\boldsymbol{\theta}_n - \hat{\boldsymbol{\theta}}_n) \quad (5)$$

with n denoting the indices where such assumption is taken. Resultingly, we can update the parameter of $q(\boldsymbol{\theta}_n)$ using as

$$\hat{\boldsymbol{\theta}}_n = \underset{\boldsymbol{\theta}_n}{\operatorname{argmax}} \langle \ln(p(\boldsymbol{\theta}|\mathbf{y})) \rangle_{q(\boldsymbol{\theta}_{-n})} \forall n \quad (6)$$

The expression (6) is formally known as the M-Step of the EM method. The remaining factored distributions not considered as point masses can be determined using (4) where the expectation with respect to $q(\boldsymbol{\theta}_n)$ would simply result in sampling $\ln(p(\boldsymbol{\theta}|\mathbf{y}))$ at $\hat{\boldsymbol{\theta}}_n$. This is formally called as the E-Step in the EM method.

Treating EM as particular case of VB allows us another advantage in addition to leveraging the existing non-minimal point estimators for the system state. It allows us the liberty to treat those parameters with point masses where the expectation evaluation with respect to that parameter would otherwise be unwieldy.

III. PROPOSED ALGORITHMS

Having chosen the two particular methods for application in robust perception tasks and having interpreted EM as a special case of VB, we are in a position to present our proposals. In this section, we first present the standard ROR method and discuss its limitations. Based on the analysis, we propose a methodology to overcome the drawbacks. Then we shift our attention to the SOR method. We present the standard SOR technique and explain its drawbacks. Based on the insights drawn, we propose two frameworks to deal with the shortcomings.

A. ROR Methods

1) *Standard ROR*: We use the version of the ROR method as originally reported in Section 2.5 of [24] where conditionally independent measurements are considered. The ROR method, as originally reported, assumes \mathbf{y}_i (measurement from each channel) to be scalar but it can be a vector in general. Accordingly, the likelihood to robustify (1) is the multivariate Student-t density. We denote the distribution as $\operatorname{St}(\mathbf{z}_s | \boldsymbol{\phi}_s, \boldsymbol{\Sigma}_s, \eta)$ where the random vector \mathbf{z}_s obeys the Student-t density and the parameters include $\boldsymbol{\phi}_s$ (mean), $\boldsymbol{\Sigma}_s$ (scale matrix) and η (degrees of freedom) which controls the kurtosis or heavy-tailedness. Resultingly, we can write the likelihood density as [24]

$$p(\mathbf{y}_i | \mathbf{x}) = \operatorname{St}(\mathbf{y}_i | \mathbf{h}_i(\mathbf{x}), \boldsymbol{\Omega}_i^{-1}, \nu_i) = \int p(\mathbf{y}_i | \mathbf{x}, \lambda_i) p(\lambda_i) d\lambda_i \quad (7)$$

with the conditional likelihood following the multivariate Gaussian density given as

$$p(\mathbf{y}_i | \mathbf{x}, \lambda_i) = \mathcal{N}(\mathbf{y}_i | \mathbf{h}_i(\mathbf{x}), (\lambda_i \boldsymbol{\Omega}_i)^{-1}) \quad (8)$$

where $\mathcal{N}(\mathbf{z}_n | \boldsymbol{\phi}_n, \boldsymbol{\Sigma}_n)$ symbolizes that the random vector \mathbf{z}_n follows the Gaussian distribution parameterized by $\boldsymbol{\phi}_n$ (mean) and $\boldsymbol{\Sigma}_n$ (covariance matrix). λ_i in (7) obeys the univariate Gamma distribution given as [24]

$$p(\lambda_i) = \mathcal{G}(\lambda_i | \frac{\nu_i}{2}, \frac{\nu_i}{2}) \quad (9)$$

where $\mathcal{G}(z_g | a_g, b_g)$ denotes that the random variable z_g follows the Gamma distribution with the shape parameter a_g and the rate parameter b_g [29]. The normalizing constant of the distribution is denoted as

$$f(a, b) = \frac{b^a}{\Gamma(a)} \quad (10)$$

where $\Gamma(a)$ denotes the Gamma function.

Denoting $\boldsymbol{\lambda}$ as the vector with λ_i its i th element, we can write the following using the Bayes theorem

$$p(\mathbf{x}, \boldsymbol{\lambda} | \mathbf{y}) \propto p(\mathbf{y} | \boldsymbol{\lambda}, \mathbf{x}) p(\mathbf{x}) p(\boldsymbol{\lambda}) \quad (11)$$

Resultingly, the log-posterior, can be written as

$$p(\mathbf{x}, \boldsymbol{\lambda} | \mathbf{y}) = \left\{ \sum_{i=1}^m \left(-0.5 \lambda_i (r_i(\mathbf{y}_i, \mathbf{x}))^2 - 0.5 \nu_i \lambda_i + (0.5(\nu_i + d) - 1) \ln(\lambda_i) \right) - 0.5 (r_0(\mathbf{y}_0, \mathbf{x}))^2 + \text{constant} \right\} \quad (12)$$

To proceed further, we seek the following VB factorization of the posterior distribution

$$p(\mathbf{x}, \boldsymbol{\lambda} | \mathbf{y}) \approx q(\mathbf{x}) q(\boldsymbol{\lambda}) \quad (13)$$

Based on (6) and (12), the state variable $\hat{\mathbf{x}}$ is estimated using the VB/EM theory as [24]

$$\hat{\mathbf{x}} = \underset{\mathbf{x} \in \mathcal{X}}{\operatorname{argmin}} \sum_{i=0}^m w_i (r_i(\mathbf{y}_i, \mathbf{x}))^2 \quad (14)$$

where $w_i = \langle \lambda_i \rangle_{q(\lambda_i)} \forall i > 0$. We have considered a point estimator for \mathbf{x} i.e. $q(\mathbf{x}) = \delta(\mathbf{x} - \hat{\mathbf{x}})$ to utilize existing solvers for spatial perception tasks mainly available in this form.

Similarly, the weights can be updated as [24]

$$w_i = \left(1 + \frac{\hat{r}_i^2 - d}{\nu + d} \right)^{-1} \quad \forall i > 0 \quad (15)$$

where d denotes the dimension of \mathbf{y}_i and $\hat{r}_i^2 = (r_i(\mathbf{y}_i, \hat{\mathbf{x}}))^2$. We assume $\nu_i = \nu \forall i$ and use w_i to weight the precision matrix instead of $\bar{\lambda}$ as in the original work to remain consistent with comparative works. Since we assume outliers occur only in the measurements, the weight for the regularizing term remains fixed as 1 i.e. $w_0 = 1$ in (14).

Limitations of standard ROR

Starting with $w_i = 1 \forall i$, the standard ROR invokes (14) and (15) iteratively till convergence. The technique has shown good performance in filtering context for different practical examples such as target tracking [24] and indoor localization [23]. This can be attributed to the appearance of well-regularized cost functions (2). However, for advanced problems in robust spatial perception, the performance of standard ROR compromises at high outlier ratios since it fails to capture the outlier characteristics by fixing ν which governs the heavy-tailedness of noise or the characteristics of outliers. Empirical evidence confirms this observation.

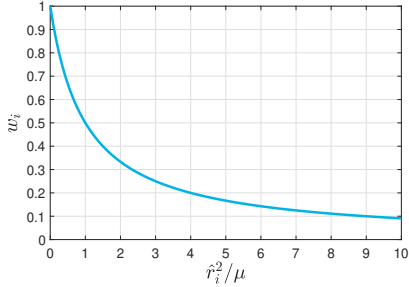


Fig. 1: w_i vs \hat{r}_i^2/μ in ROR.

For further understanding of this limitation consider how w_i changes with parameters of Student-t distribution. The variation of w_i against \hat{r}_i^2/μ is shown in Fig. 1 where $\mu = \nu + d$. The plot of (15) would only be a shifted version of the plot in Fig. 1. Since $\hat{r}_i^2 \gg d$ when outlier appears in the i th dimension, we can simplify (15) as $w_i = (1 + \frac{\hat{r}_i^2}{\mu})^{-1}$ indicating the importance of the kurtosis ν and resultingly μ . It can be observed that the residuals are gradually downweighted with increasing magnitude during estimation with $w_i = 0.5$ for $\hat{r}_i^2 = \mu$. Since the residuals are evaluated considering the state estimate using all the measurements initially, it is possible that the squared residuals even for the uncorrupted dimensions become greater than the prefixed μ downweighting them in the process. This can lead to performance issues. Therefore, this calls for adapting μ by considering the residuals evaluated with clean and corrupted measurements. Given the limitations, we propose a variant of the standard ROR method where μ is adapted during iterations considering the residuals at each iteration. We call it Extended ROR or simply EROR.

2) *EROR*: In EROR, we propose adaptation of μ during iterations considering the updated squared residuals based on the relationship of the w_i and μ . The choice of μ is done such that weights assigned to residuals span the maximum portion of the zero to one range. In other words, the largest residuals need to be pruned with the smallest weights in the weighted least squared cost function and vice versa. In particular, for $\hat{r}_i^2 = \hat{r}_{\max}^2$ with $w_i \rightarrow 0$ leads to $\mu \rightarrow 0$ ($\mu = \frac{\hat{r}_i^2}{1/w_i - 1}$). Practically, $\mu \ll \hat{r}_{\max}^2$. Similarly for the other extreme $\hat{r}_i^2 = \hat{r}_{\min}^2$ with $w_i \rightarrow 1$ leads to $\mu \rightarrow \infty$. Practically, $\mu \gg \hat{r}_{\min}^2$. To cater for both extremes we propose $\mu = \text{mean}(\hat{r}_{\max}^2, \hat{r}_{\min}^2)$. Also, μ is lower bounded by χ to ensure residuals within a minimum threshold are not neglected during estimation. The notion of χ is similar to \bar{c}^2 as in [11] which is set as the

maximum error expected for the inliers. Note that adaptation of μ is intuitive which can be viewed as an additional step in the standard ROR devised using VB. EROR is presented as Algorithm 1.

Algorithm 1: EROR

```

Initialize  $w_i = 1 \forall i$ 
while the convergence criterion has not met do
    Variable update:  $\hat{\mathbf{x}} = \underset{\mathbf{x} \in \mathcal{X}}{\text{argmin}} \sum_i w_i (r_i(\mathbf{y}_i, \mathbf{x}))^2$ 
    Residual update:  $\hat{r}_i^2 = (r_i(\mathbf{y}_i, \hat{\mathbf{x}}))^2 \forall i$ 
    Parametric update:
         $\hat{r}_{\max}^2 = \max_i(\hat{r}_i^2); \hat{r}_{\min}^2 = \min_i(\hat{r}_i^2)$  s.t.  $i > 0$ 
         $\mu = \max(\text{mean}(\hat{r}_{\max}^2, \hat{r}_{\min}^2), \chi)$ 
    Weight update:  $w_i = \frac{1}{1 + (\hat{r}_i^2/\mu)} \forall i > 0$ 
end

```

B. SOR Methods

1) *Standard SOR*: The SOR method, as originally reported [23], assumes \mathbf{y}_i to be scalar but it can be a vector in general. In the original work, an indicator vector $\mathcal{I} \in \mathbb{R}^m$ with Bernoulli elements is introduced to describe outliers in the measurements. In particular, $\mathcal{I}_i = \epsilon$ indicates the occurrence of an outlier in the i th dimension and $\mathcal{I}_i = 1$ is reserved for the no outlier case. Accordingly, the conditional likelihood to robustify (1) is a multivariate Gaussian density function [23]

$$\begin{aligned}
 p(\mathbf{y}_i | \mathbf{x}, \mathcal{I}_i) &= \mathcal{N}(\mathbf{y}_i | \mathbf{h}_i(\mathbf{x}), (\mathcal{I}_i \boldsymbol{\Omega}_i)^{-1}) \\
 &= \frac{1}{\sqrt{(2\pi)^m |\boldsymbol{\Omega}_i^{-1}|}} e^{(-0.5 \mathcal{I}_i (r_i(\mathbf{y}_i, \mathbf{x}))^2) \mathcal{I}_i^{0.5}} \quad (16)
 \end{aligned}$$

$\mathcal{I}_i \forall i > 0$ is assumed to have the following prior distribution

$$p(\mathcal{I}_i) = (1 - \theta_i) \delta(\mathcal{I}_i - \epsilon) + \theta_i \delta(\mathcal{I}_i - 1) \quad (17)$$

where θ_i denotes the prior probability of having no outlier in the i th measurement channel. ϵ has the role of catering for describing the anomalous data in effect controlling the covariance of outliers. Using the Bayes theorem we can write

$$p(\mathbf{x}, \mathcal{I} | \mathbf{y}) \propto p(\mathbf{y} | \mathcal{I}, \mathbf{x}) p(\mathbf{x}) p(\mathcal{I}) \quad (18)$$

where \mathcal{I} denotes the vector with \mathcal{I}_i its i th element.

As a result, the log-posterior is given as

$$\begin{aligned}
 \ln(p(\mathbf{x}, \mathcal{I}, \mathbf{y})) &= \left\{ \sum_{i=1}^m \left(-0.5 \mathcal{I}_i (r_i(\mathbf{y}_i, \mathbf{x}))^2 + 0.5 \ln(\mathcal{I}_i) \right) \right. \\
 &+ \ln \left((1 - \theta_i) \delta(\mathcal{I}_i - \epsilon) + \theta_i \delta(\mathcal{I}_i - 1) \right) - 0.5 (r_0(\mathbf{y}_0, \mathbf{x}))^2 \\
 &\left. + \text{constant} \right\} \quad (19)
 \end{aligned}$$

For tractable inference we resort to the following VB factorization of the posterior distribution

$$p(\mathbf{x}, \mathcal{I} | \mathbf{y}) \approx q(\mathbf{x}) q(\mathcal{I}) \quad (20)$$

Based on (6) and (19), the state estimate $\hat{\mathbf{x}}$ is updated using the VB/EM theory as [23]

$$\hat{\mathbf{x}} = \underset{\mathbf{x} \in \mathcal{X}}{\operatorname{argmin}} \sum_{i=0}^m w_i (r_i(\mathbf{y}_i, \mathbf{x}))^2 \quad (21)$$

with $w_0 = 1$ and

$$w_i = \langle \mathcal{I}_i \rangle_{q(\mathcal{I}_i)} \quad \forall i > 0 \quad (22)$$

$$= \Omega_i + (1 - \Omega_i)\epsilon \approx \Omega_i \quad (23)$$

where Ω_i parameterizes the VB posterior marginal $q(\mathcal{I}_i)$ corresponding to θ_i in $p(\mathcal{I}_i)$. Ω_i is updated using (4) and (19) as [23]

$$\Omega_i = \frac{1}{1 + \sqrt{\epsilon} \left(\frac{1}{\theta_i} - 1 \right) e^{(0.5 \hat{r}_i^2 (1 - \epsilon))}} \quad (24)$$

Since the hyperparameter ϵ is assumed to be a small positive number we denote it as $\epsilon = \exp(-\rho^2)$. Assuming a neutral prior for the occurrence of an outlier in the i th dimension i.e. $\theta_i = 0.5$ (as reported originally [23]) and noting that $\epsilon = \exp(-\rho^2) \approx 0$ we can write

$$w_i \approx \Omega_i \approx \frac{1}{1 + e^{(0.5(\hat{r}_i^2 - \rho^2))}} \quad \forall i > 0 \quad (25)$$

Limitations of standard SOR

Starting with $w_i = 1 \quad \forall i$, the standard SOR invokes (21) and (25) iteratively till convergence. The technique has shown good performance in the filtering context [23] but has limited ability in robust spatial perception tasks as the standard ROR method. This drawback compromises the performance especially at high outlier ratios since the standard SOR fails to capture the outlier characteristics by fixing ρ^2 (or ϵ) which governs the covariance of outliers. Experimental evidence verifies this limitation.

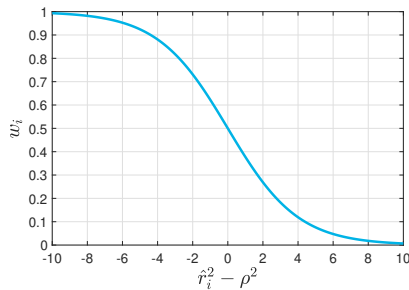


Fig. 2: w_i vs $\hat{r}_i^2 - \rho^2$ in SOR.

To further appreciate this limitation consider how w_i changes with $\hat{r}_i^2 - \rho^2$ as shown in Fig. 2. It can be observed that the residuals are gradually downweighted with increasing magnitude during estimation with $w_i = 0.5$ for $\hat{r}_i^2 = \rho^2$. Since the residuals are evaluated considering the state estimate using all the measurements initially, it is possible that the squared residuals even for the uncorrupted dimensions become greater than the prefixed ρ^2 downweighting them during the inference process. This can lead to performance issues. Therefore, this calls for adapting ρ^2 by considering the residuals evaluated with clean and corrupted measurements.

Given the limitations, we present two methods based on the standard SOR technique. Firstly, we propose a modification in the SOR method by explicitly adapting ρ^2 during iterations considering the residuals at each iteration. We call it Extended SOR or simply ESOR. Secondly, by modifying the basic SOR model with a notion of adaptive unknown covariance of outliers, we propose Adaptive SOR or simply ASOR where the parameters controlling the covariance of outliers are *learned* within the inferential procedure.

2) *ESOR*: In ESOR, we modify ρ^2 during iterations taking into account the updated squared residuals. In particular, we propose to select $\rho^2 = \sum_{i=0}^m w_i \hat{r}_i^2 / \sum_{i=0}^m w_i$. In other words, ρ^2 is selected as the effective centroid of points given as squared residuals considering the weights assigned. With such an intuitive choice, the probability of declaring an outlier in the i th dimension is 0.5 when \hat{r}_i^2 equals the effective mean of squared residuals. The residuals greater than ρ become the candidates for downweighting and vice versa during an iteration. Lastly, ρ^2 is lower bounded by γ to ensure residuals within a minimum threshold are not neglected during estimation. ESOR is presented as Algorithm 2.

Algorithm 2: ESOR

Initialize $w_i = 1 \quad \forall i$

while the convergence criterion has not met **do**

Variable update: $\hat{\mathbf{x}} = \underset{\mathbf{x} \in \mathcal{X}}{\operatorname{argmin}} \sum_i w_i (r_i(\mathbf{y}_i, \mathbf{x}))^2$

Residual update: $\hat{r}_i^2 = (r_i(\mathbf{y}_i, \hat{\mathbf{x}}))^2 \quad \forall i$

Parameteric update: $\rho^2 = \max\left(\frac{\sum_i w_i \hat{r}_i^2}{\sum_i w_i}, \gamma\right)$

Weight update: $w_i = \frac{1}{1 + e^{(0.5(\hat{r}_i^2 - \rho^2))}} \quad \forall i > 0$

end

3) *ASOR*: For devising ESOR we adapt ρ^2 (or ϵ) during iterations to capture the characteristics of outliers. Nevertheless, the choice of selection of ρ^2 which controls the covariance of outliers is entirely intuitive. This can be viewed as an additional step within the standard SOR method, not falling under the standard VB approach. However, the insights drawn from ESOR with sound experimental performance suggest the merits of considering or *learning* the characteristics of outliers during inference. With these observations, we now present ASOR which is devised with the standard VB approach. In contrast to EROR and ESOR, we jointly *estimate* the covariance controlling factor along with the state and the weights in ASOR.

The conditional likelihood for designing ASOR remains same as for the standard SOR given in (16). Building on the insights from EROR and ESOR, we need to adapt covariances to describe the outliers. In particular, we assume that for outlier occurrence in the i th observation channel i.e. $\mathcal{I}_i \neq 1$ in (16), \mathcal{I}_i obeys a Gamma probability density being supported on the set of positive real numbers. Resultingly, we write the hierarchical prior distribution of \mathcal{I}_i given as

$$p(\mathcal{I}_i | b) = (1 - \theta_i) \underbrace{f(a, b) \mathcal{I}_i^{a-1} e^{-b\mathcal{I}_i}}_{\mathcal{G}(\mathcal{I}_i | a, b)} + \theta_i \delta(\mathcal{I}_i - 1) \quad (26)$$

where we assume the two components of $p(\mathcal{I}_i|b)$ in (26) as disjoint with the Gamma density defined as zero for $\mathcal{I}_i = 1$ without losing anything. This assumption helps in subsequent derivation. The parameter b is the factor that captures the common effect of outliers in each observation channel. From the Bayesian theory we know that the conjugate prior of b is also a Gamma distribution given as [30]

$$p(b) = f(A, B)b^{A-1}e^{-Bb} \quad (27)$$

where A and B are the parameters of this Gamma distribution. We are now in a position to invoke the Bayes theorem given as

$$p(\mathbf{x}, \mathcal{I}, b|\mathbf{y}) \propto p(\mathbf{y}|\mathcal{I}, \mathbf{x})p(\mathbf{x})p(\mathcal{I}|b)p(b) \quad (28)$$

Resultingly, the log-posterior, which is used in subsequently derivation, is given as

$$\begin{aligned} \ln(p(\mathbf{x}, \mathcal{I}, b|\mathbf{y})) = & \left\{ \sum_{i=1}^m \left(-0.5\mathcal{I}_i(r_i(\mathbf{y}_i, \mathbf{x}))^2 + 0.5 \ln(\mathcal{I}_i) \right. \right. \\ & + \ln((1 - \theta_i)f(a, b)\mathcal{I}_i^{a-1}e^{-b\mathcal{I}_i} + \theta_i\delta(\mathcal{I}_i - 1)) \left. \right\} \\ & - 0.5(r_0(\mathbf{y}_0, \mathbf{x}))^2 + (A - 1) \ln(b) - Bb + \text{constant} \left. \right\} \quad (29) \end{aligned}$$

To proceed further we resort to the VB factorization given as

$$p(\mathbf{x}, \mathcal{I}, b|\mathbf{y}) \approx q(\mathbf{x})q(\mathcal{I})q(b) \quad (30)$$

Using the VB/EM theory and with the assumption that $q(\mathbf{x}) = \delta(\mathbf{x} - \hat{\mathbf{x}})$ we obtain the following using (6) and (29)

$$\hat{\mathbf{x}} = \underset{\mathbf{x} \in \mathcal{X}}{\operatorname{argmin}} \sum_{i=0}^m w_i(r_i(\mathbf{y}_i, \mathbf{x}))^2 \quad (31)$$

where $w_0 = 1$ and

$$w_i = \langle \mathcal{I}_i \rangle_{q(\mathcal{I}_i)} \quad \forall i > 0 \quad (32)$$

Thanks to the notion of VB-conjugacy [27], it turns out that $q(\mathcal{I}_i)$ has a same functional form as of $p(\mathcal{I}_i|b)$ in (26). $q(\mathcal{I}_i)$ is parameterized by α , β_i and Ω_i corresponding to a , b and θ_i in $p(\mathcal{I}_i|b)$ respectively. Resultingly, we can evaluate the expectation in (32) as

$$w_i = \Omega_i + (1 - \Omega_i)\alpha/\beta_i \quad \forall i > 0 \quad (33)$$

The VB marginal $q(\mathcal{I})$ can be obtained using (4) and (29) as

$$\begin{aligned} q(\mathcal{I}) \propto & \prod_{i=1}^m \left\{ \mathcal{I}_i^{0.5} e^{-0.5\hat{r}_i^2 \mathcal{I}_i} ((1 - \theta_i)f(a, b)\mathcal{I}_i^{a-1}e^{-\hat{b}\mathcal{I}_i} \right. \\ & \left. + \theta_i\delta(\mathcal{I}_i - 1)) \right\} \quad (34) \end{aligned}$$

where we have assume a point estimator for b i.e. $q(b) = \delta(b - \hat{b})$ to simplify the arising expectations.

We can further write

$$\begin{aligned} q(\mathcal{I}) = & \prod_{i=1}^m \left\{ k_i(1 - \theta_i)f(a, \hat{b})\mathcal{I}_i^{\alpha-1}e^{-\beta_i\mathcal{I}_i} + \right. \\ & \left. k_i\theta_i e^{-0.5\hat{r}_i^2} \delta(\mathcal{I}_i - 1) \right\} \quad (35) \end{aligned}$$

where k_i is the proportionality constant for the i th dimension, $\beta_i = 0.5\hat{r}_i^2 + \hat{b}$ and $\alpha = a + 0.5$.

Proceeding ahead we can write

$$q(\mathcal{I}) = \prod_{i=1}^m \overbrace{(1 - \Omega_i) \underbrace{f(\alpha, \beta_i)\mathcal{I}_i^{\alpha-1}e^{-\beta_i\mathcal{I}_i}}_{q^1(\mathcal{I}_i)} + \Omega_i\delta(\mathcal{I}_i - 1)}^{q(\mathcal{I}_i)} \quad (36)$$

where

$$\Omega_i = k_i e^{-0.5\hat{r}_i^2} \theta_i \quad (36)$$

To determine k_i , we note that the distribution in (35) should integrate to 1. Therefore, the following should hold

$$k_i\theta_i e^{-0.5\hat{r}_i^2} + k_i(1 - \theta_i) \frac{f(a, \hat{b})}{f(\alpha, \beta_i)} = 1 \quad (37)$$

Leading to

$$k_i = \frac{1}{\theta_i e^{-0.5\hat{r}_i^2} + (1 - \theta_i) \frac{f(a, \hat{b})}{f(\alpha, \beta_i)}} \quad (38)$$

Resultingly, using (10) and (36), (38) we arrive at

$$\Omega_i = \frac{1}{1 + \zeta \frac{\hat{b}^\alpha}{\beta_i^\alpha} e^{0.5\hat{r}_i^2}} \quad \forall i > 0 \quad (39)$$

where $\zeta = (\frac{1}{\theta_i} - 1) \frac{\Gamma(\alpha)}{\Gamma(a)}$.

Lastly, in a similar manner using the VB/EM approach we can determine $q(b) = \delta(b - \hat{b})$ where using (6) and (29)

$$\hat{b} = \underset{b}{\operatorname{argmax}} \langle \ln(p(\hat{\mathbf{x}}, \mathcal{I}, b|\mathbf{y})) \rangle_{q(\mathcal{I})} \quad (40)$$

The expected log-posterior in (40) can be written as

$$\begin{aligned} \langle \ln(p(\hat{\mathbf{x}}, \mathcal{I}, b|\mathbf{y})) \rangle_{q(\mathcal{I})} = & \left\{ \sum_{i=1}^m v_i(b) + (A - 1) \ln(b) - Bb \right. \\ & \left. + \text{constant} \right\} \quad (41) \end{aligned}$$

where

$$v_i(b) = \langle \ln((1 - \theta_i)f(a, b)\mathcal{I}_i^{a-1}e^{-b\mathcal{I}_i} + \theta_i\delta(\mathcal{I}_i - 1)) \rangle_{q(\mathcal{I}_i)} \quad (42)$$

which can further be written as follows considering only the terms dependent on b

$$v_i(b) = (1 - \Omega_i)(\ln(f(a, b)) - b\langle \mathcal{I}_i \rangle_{q^1(\mathcal{I}_i)}) + \text{constant} \quad (43)$$

where we assume $q^1(\mathcal{I}_i)$ is defined as zero for $\mathcal{I}_i = 1$ as the prior Gamma density in (26). Given $\langle \mathcal{I}_i \rangle_{q^1(\mathcal{I}_i)} = \alpha/\beta_i$ and using the expressions in (10) and (43), we can write (41) as

$$\langle \ln(p(\hat{\mathbf{x}}, \mathcal{I}, b|\mathbf{y})) \rangle_{q(\mathcal{I})} = (\bar{A} - 1) \ln(b) - \bar{B}b + \text{constant} \quad (44)$$

where

$$\bar{A} = A + \sum_{i=1}^m a(1 - \Omega_i) \quad (45)$$

$$\bar{B} = B + \sum_{i=1}^m (1 - \Omega_i) \frac{\alpha}{\beta_i} \quad (46)$$

Maximizing (44) using differentiation, we obtain \hat{b} according to (40) as

$$\hat{b} = \frac{\bar{A} - 1}{B} \quad \text{s.t.} \quad \bar{A} > 1 \quad (47)$$

where $\bar{A} > 1$ owing to the requirement of positivity of parameter b of Gamma distribution in (26) being approximated in (47). Also noting that the parameter $a > 0$ for validity of the Gamma distribution in (26), $A > 1$ is a sufficient condition for (47) to hold considering (45). Lastly, note that since the rate parameter of distribution in (27) is positive i.e. $B > 0$ any numerical errors in (47) are avoided. The resulting method namely ASOR is given as Algorithm 3.

Algorithm 3: ASOR

Initialize $w_i = 1 \forall i$ and $A, B, a, \hat{b}, \theta_i \forall i$
 Evaluate $\alpha = a + 0.5$ and $\zeta = (\frac{1}{\theta_i} - 1) \frac{\Gamma(\alpha)}{\Gamma(a)}$
while the convergence criterion has not met **do**
 Variable update: $\hat{\mathbf{x}} = \underset{\mathbf{x} \in \mathcal{X}}{\text{argmin}} \sum_i w_i (r_i(\mathbf{y}_i, \mathbf{x}))^2$
 Residual update: $\hat{r}_i^2 = (r_i(\mathbf{y}_i, \hat{\mathbf{x}}))^2 \forall i$
 Parameteric updates:
 $\beta_i = 0.5 \hat{r}_i^2 + \hat{b}$
 $\Omega_i = \frac{1}{1 + \zeta \frac{\hat{b}^\alpha}{\beta_i^\alpha} e^{0.5 \hat{r}_i^2}}$
 $\hat{b} = \frac{A - 1 + \sum_i a(1 - \Omega_i)}{B + \sum_i (1 - \Omega_i) \frac{a}{\beta_i}}$
 Weight update: $w_i = \Omega_i + (1 - \Omega_i) \alpha / \beta_i \forall i > 0$
end

Remarks

It is interesting to note that the variable update steps in EROR, ESOR and ASOR is the same as in GNC reflecting their ability to employ non-minimal solvers during inference. We propose using the change in $\sum_i w_i \hat{r}_i^2$ during consecutive iterations as the standard convergence criterion. We lastly remark that in EROR and ESOR an exception to break the iterations can be added for seamless operation when the sum of the weights gets close to zero which we experienced in certain applications with very high ratios of outliers.

IV. EXPERIMENTS

In this section, we discuss the performance results of the proposed methods for different spatial perception applications including 3D point cloud registration (code: MATLAB), mesh registration (code: MATLAB), and pose graph optimization (PGO) (code: C++) on an Intel i7-8550U processor-based computer and consider SI units. We consider GNC-GM and GNC-TLS as the benchmark methods which have shown good results in these applications outperforming methods including the classical RANSAC and recently introduced ADAPT. For EROR and ESOR we consider $\chi = \gamma = \bar{c}^2$ where \bar{c}^2 , dictating the maximum error expected for the inliers, is set as specified in the original work [11]. In ASOR we resort to the choice of initialization which performs the best across different applications given as $a = 0.5, A = 10000, B = 1000, \hat{b} =$

10000, $\theta_i = 0.5 \forall i$. We use the normalized incremental change of 10^{-5} in $\sum_i w_i \hat{r}_i^2$ during consecutive iterations as the convergence criterion for GNC-TLS, EROR, ESOR and ASOR. For GNC-GM the convergence criterion remains the same as originally reported.

A. 3D Point Cloud Registration

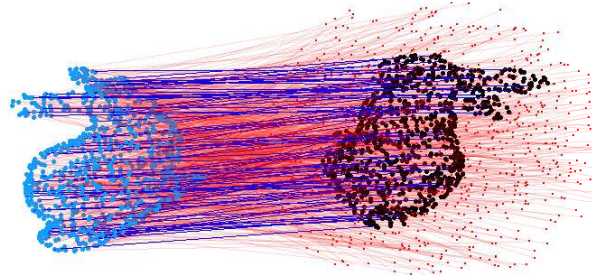


Fig. 3: Point clouds with correspondences in 3D point cloud registration for the *Bunny* dataset [31].

In 3D point cloud registration, we assume that a set of 3D points $\mathbf{p}_i \in \mathbb{R}^3, i = 1, \dots, m$ undergo a transformation, with rotation $\mathbf{R} \in \text{SO}(3)$ and translation $\mathbf{t} \in \mathbb{R}^3$, resulting in another set of 3D points $\mathbf{q}_i \in \mathbb{R}^3, i = 1, \dots, m$. The putative correspondences $(\mathbf{p}_i, \mathbf{q}_i)$ can be potentially infested with outliers. Fig. 3 depicts how the *Bunny* point cloud from the Stanford repository [31] undergoes a random transformation in a point cloud registration setup (blue lines: inliers, red lines: outliers). The objective is to estimate \mathbf{R} and \mathbf{t} that best aligns the two point clouds by minimizing the effect of outliers. The problem can be cast in form of (2) where the i th residual is the Euclidean distance between \mathbf{q}_i and $\mathbf{R}\mathbf{p}_i + \mathbf{t}$. We resort to the renowned Horn’s method as the non-minimal solver for this case which provides closed form estimates in the outlier-free case [8].

Using the proposed EROR, ESOR and ASOR we robustify the Horn’s method and report the results for the *Bunny* dataset. We downsample the point cloud to $m = 100$ points and restrict it within a $[-0.5, 0.5]^3$ box before applying a random rotation $\mathbf{R} \in \text{SO}(3)$ and a random translation \mathbf{t} ($\|\mathbf{t}\|_2 \leq 3$). The inliers of the transformed points are corrupted with independent noise samples drawn from $\mathcal{N}(0, 0.001^2)$ whereas the outliers are randomly generated being contained within a sphere of diameter $\sqrt{3}$. 20 Monte Carlo (MC) runs are used to capture the error statistics for up to 90% outlier contamination ratio.

Figs. 4 showcase the performance results of our proposed methods in comparison to the GNC methods. The rotation and translational error statistics as depicted in Figs. 4a-4b are very similar in all the cases with errors generally increasing for all the methods at large outlier ratios. In terms of computational complexity, the gains of the Bayesian heuristics can be observed for this case in Fig. 4c which is a key evaluation parameter for runtime performance. ESOR exhibits much faster comparative behavior followed by EROR and ASOR for the entire range of outlier ratios. We have observed similar error performance of the methods for other values of m (upto maximum number of available points). Also we have

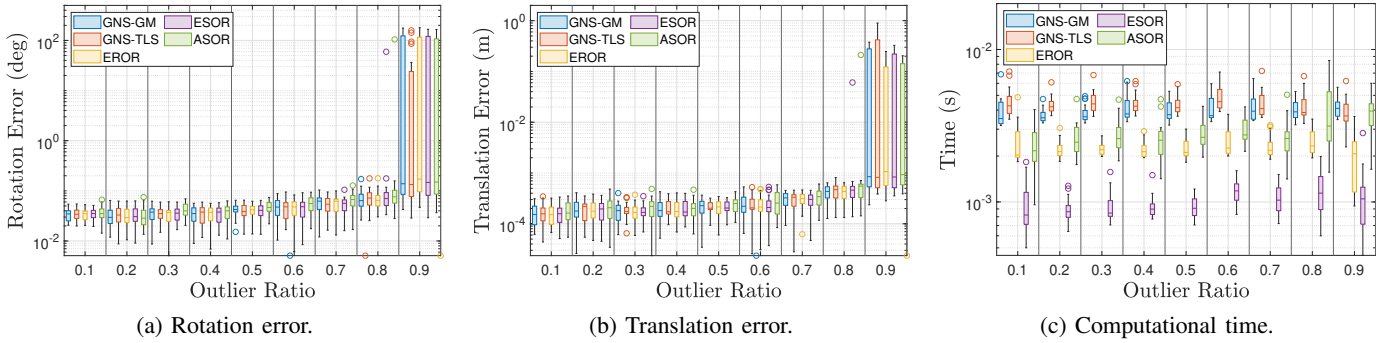


Fig. 4: Performance of robust estimators for 3D point cloud registration considering the *Bunny* dataset [31].

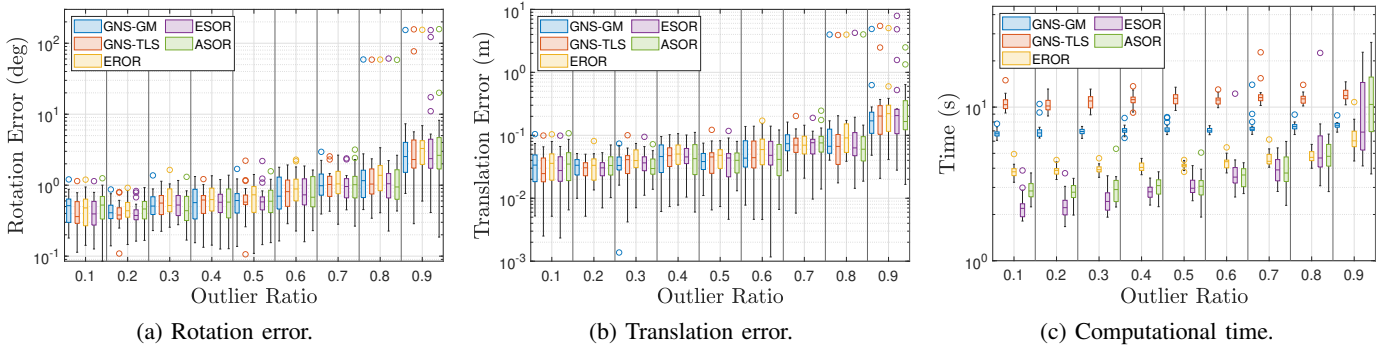


Fig. 5: Performance of robust estimators for mesh registration considering the *motorbike* model [32].

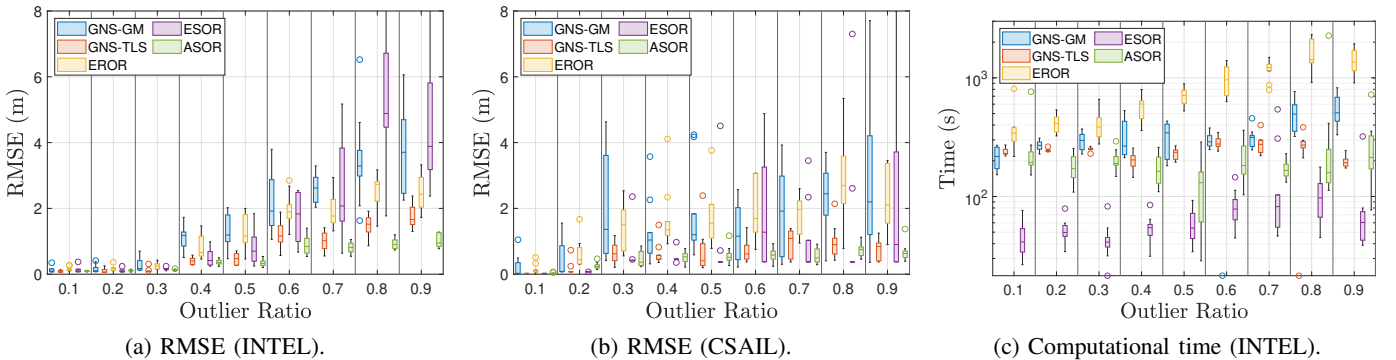


Fig. 6: Performance of robust estimators for pose graph optimization considering Intel and CSAIL datasets.

noticed that with an increase in the inlier noise magnitude and number of points, ASOR slows down becoming computationally comparative to the GNC methods. Moreover, we have noted that increasing the parameter a generally reduces the processing time at the cost of slightly increased errors at higher outlier ratios.

Other specialized solvers like TEASER [33] also exist for point cloud registration problems which are certifiably robust and can sustain higher outlier contamination better. However, it has scalability issues thanks to the involvement of sluggish semidefinite programming (SDP) based solution for rotation estimation. An improved version of TEASER namely TEASER++ [18] was recently introduced that leverages the heuristic, GNC-TLS, in its inferential pipeline for rotation estimation while still certifying the estimates. Owing to the well-devised estimation pipeline, GNC-TLS has to deal with

a smaller percentage of outliers making TEASER++ faster and improving its practicality. Since the error performance of the Bayesian heuristics is similar to the GNC methods and these are generally found to be faster in various scenarios of the point cloud registration problem this indicates their utility as standalone estimators. Moreover, these can potentially be useful in other inferential pipelines like TEASER++ (while enjoying certifiable performance) but need a thorough evaluation.

B. Mesh registration

In the mesh registration problem, the points \mathbf{p}_i from the a point cloud are transformed to general 3D primitives \mathbf{q}_i including points, lines, and/or planes. Fig. 7 shows the result of a random transformation of a point cloud to the *motorbike* mesh model from the PASCAL dataset [32] (blue lines: inliers,

red lines: outliers). The aim is to estimate the \mathbf{R} and \mathbf{t} by minimizing the squared sum of residuals which represent the corresponding distances. We resort to [9] as the basic non-minimal solver which has been proposed to find the globally optimal solution for the outlier-free case. Using the presented EROR,

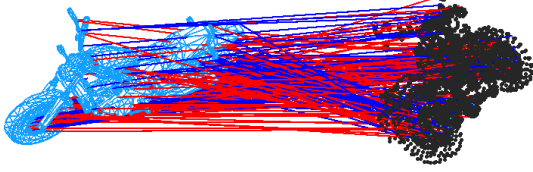


Fig. 7: Mesh and point cloud with correspondences in mesh registration for the *motorbike* mesh model [32]

ESOR and ASOR heuristics we robustify the solver and report the results for the *motorbike* mesh model. To create point cloud we randomly sample points on the vertices, edges and faces of the mesh model, and then apply a random transformation ($\mathbf{R} \in \text{SO}(3)$, \mathbf{t} ($\|\mathbf{t}\|_2 \leq 5$)) and subsequently add independent noise samples from $\mathcal{N}(0, 0.01^2)$. Considering 100 point-to-point, 80 point-to-line and 80 point-to-plane correspondences, we create outliers by random erroneous correspondences. For this case also, 20 MC runs are carried out to generate the error statistics for up to 90% outlier contamination ratio. We see a trend similar to the point cloud registration case as depicted in Figs. 5a-5b. In particular, the performance in terms of errors is similar for all the algorithms. However, the Bayesian heuristics exhibit a general computational advantage, except at very high outlier ratios where the performance becomes comparable. The Bayesian heuristics generally have similar runtimes with SOR modifications having a general advantage. We observed similar performance of the methods for other combinations of correspondences in this case.

During the experiments of point cloud and mesh registration, we have noticed that ROR and SOR modifications generally get computationally more advantageous, with estimation quality remaining similar, when the outliers become larger in comparison to the nominal noise samples.

C. Pose graph optimization

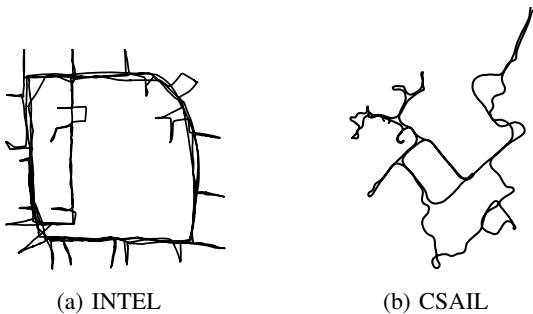


Fig. 8: Ground truth paths of datasets considered in pose graph optimization.

PGO is typically employed for several problems arising in robotic and computer vision applications like SLAM and

structure from motion (SfM) [34]. The objective is to estimate a set of poses $(\mathbf{t}_i, \mathbf{R}_i), i = 1, \dots, m$ using pairwise relative measurements $(\mathbf{t}_{ij}, \mathbf{R}_{ij})$. Relative observations can result in consecutive pose constraints (e.g. from odometry measurements) or non-successive pose constraints (e.g. from scan matalphang) also known as loop closures. The residual error for this case is given as

$$r(\mathbf{R}_i, \mathbf{t}_i) = \sqrt{\kappa_{ij} \|\mathbf{R}_j - \mathbf{R}_i \tilde{\mathbf{R}}_{ij}\|_F^2 + \tau_{ij} \|\mathbf{t}_j - \mathbf{t}_i - \mathbf{R}_i \tilde{\mathbf{t}}_{ij}\|_2^2}$$

where κ_{ij} and τ_{ij} encode the measurement noise statistics and $\|\cdot\|_F$ denotes the Frobenius norm. We resort to SE-Sync [10] as the non-minimal solver for this case and use the Python binding of C++ open-sourced by the authors. Adopting the same experimentation setup of GNC we randomly corrupt loop closures and retain odometry observations. For benchmarking we consider 2D datasets including INTEL and CSAIL which are available openly (path ground truth plotted in Fig. 8). Since simulations take much more time as compared to the previous case we carry out 10 MC runs to obtain the error statistics. Fig. 6a showcases the root mean squared (RMSE) of the trajectory considering the INTEL dataset. The proposed Bayesian heuristics in this case also exhibit comparative performance to the GNC methods. At very higher outlier rates ESOR has slightly compromised performance. In Fig. 6b the RMSE for the CSAIL dataset are depicted reflecting the same pattern. In the PGO examples, GNC-TLS and ASOR outperform other methods with ASOR generally having the least error for different outlier ratios. As far as the computational performance is concerned ESOR has the smallest runtime, followed by ASOR while ROR is the slowest for both cases. Fig. 6c depicts the computational runtime statistics for the INTEL dataset. CSAIL has similar computational time statistics with ESOR being relatively much faster as compared to other methods.

Lastly, we also evaluated the Bayesian heuristics using $\max_i (w^i \hat{r}_i^2) < \bar{c}^2$ as the stopping criteria which resulted in much faster performance but with slightly degraded error performance in the considered scenarios of the spatial perception applications.

V. CONCLUSION

We have proposed three Bayesian heuristics: EROR, ESOR and ASOR as nonlinear estimators for spatial perception problems. Like the existing general-purpose GNC heuristics, these have the ability to invoke existing non-minimal solvers. Evaluations in several experiments demonstrate their merits as compared to the GNC heuristics. In particular, in the 3D point cloud and mesh registration problems EROR, ESOR and ASOR have similar estimation errors over a wide range of outlier ratios. However, the Bayesian heuristics have a general advantage in computational terms. For the PGO setups, we generally find the Bayesian methods to compete with GNC in estimation quality. The devised ROR and SOR modifications are found to be the least and most computationally efficient for this case. Using another suggested criteria can lead to further improvement in computational terms at expense of estimation quality. In short, the proposed methods provide general purpose options, in addition to the GNC heuristics,

to robustify the existing non-minimal solvers against outliers in different spatial perception applications indicating their usefulness. Empirical evidence suggests that the proposed approaches provide a general edge in computational terms while remaining competitive in terms of error. The actual possible gains depend on whether the solvers are used standalone or in an inferential pipeline for the particular application scenarios and should be evaluated for the case under consideration before deployment. We believe that the work can be further extended in different directions by aiming to devise the heuristics without knowledge of nominal noise statistics. Moreover, these methods can also be tested within hybrid approaches where the estimates subsequently get certified for optimality.

REFERENCES

- [1] B. Drost, M. Ulrich, N. Navab, and S. Ilic, "Model globally, match locally: Efficient and robust 3D object recognition," in *2010 IEEE Computer Society Conference on Computer Vision and Pattern Recognition*, 2010, pp. 998–1005.
- [2] D. Scaramuzza and F. Fraundorfer, "Visual odometry [tutorial]," *IEEE Robotics and Automation Magazine*, vol. 18, no. 4, pp. 80–92, 2011.
- [3] C. Cadena, L. Carlone, H. Carrillo, Y. Latif, D. Scaramuzza, J. Neira, I. Reid, and J. J. Leonard, "Past, present, and future of simultaneous localization and mapping: Toward the robust-perception age," *IEEE Transactions on Robotics*, vol. 32, no. 6, pp. 1309–1332, 2016.
- [4] Y.-Q. Liu, F. Jin, K.-F. Dong, J.-L. Song, W.-Q. Mo, and Y.-J. Hui, "Eccentric optimization of multisensor for SLAM-integrated navigation," *IEEE Transactions on Instrumentation and Measurement*, vol. 72, pp. 1–8, 2023.
- [5] A. H. Chughtai, M. Tahir, and M. Uppal, "A robust Bayesian approach for online filtering in the presence of contaminated observations," *IEEE Transactions on Instrumentation and Measurement*, vol. 70, pp. 1–15, 2021.
- [6] P. Antonante, V. Tzoumas, H. Yang, and L. Carlone, "Outlier-robust estimation: Hardness, minimally tuned algorithms, and applications," *IEEE Transactions on Robotics*, vol. 38, no. 1, pp. 281–301, 2022.
- [7] J. Wang, Z. Meng, and L. Wang, "Efficient probabilistic approach to range-only SLAM with a novel likelihood model," *IEEE Transactions on Instrumentation and Measurement*, vol. 70, pp. 1–12, 2021.
- [8] B. K. Horn, "Closed-form solution of absolute orientation using unit quaternions," *Josa a*, vol. 4, no. 4, pp. 629–642, 1987.
- [9] J. Briales and J. Gonzalez-Jimenez, "Convex global 3D registration with Lagrangian duality," in *2017 IEEE Conference on Computer Vision and Pattern Recognition (CVPR)*, 2017, pp. 5612–5621.
- [10] D. M. Rosen, L. Carlone, A. S. Bandeira, and J. J. Leonard, "Se-sync: A certifiably correct algorithm for synchronization over the special euclidean group," *The International Journal of Robotics Research*, vol. 38, no. 2-3, pp. 95–125, 2019.
- [11] H. Yang, P. Antonante, V. Tzoumas, and L. Carlone, "Graduated non-convexity for robust spatial perception: From non-minimal solvers to global outlier rejection," *IEEE Robotics and Automation Letters*, vol. 5, no. 2, pp. 1127–1134, 2020.
- [12] M. A. Fischler and R. C. Bolles, "Random sample consensus: a paradigm for model fitting with applications to image analysis and automated cartography," *Communications of the ACM*, vol. 24, no. 6, pp. 381–395, 1981.
- [13] V. Tzoumas, P. Antonante, and L. Carlone, "Outlier-robust spatial perception: Hardness, general-purpose algorithms, and guarantees," in *2019 IEEE/RSJ International Conference on Intelligent Robots and Systems (IROS)*, 2019, pp. 5383–5390.
- [14] J. L. Schonberger and J.-M. Frahm, "Structure-from-motion revisited," in *Proceedings of the IEEE Conference on Computer Vision and Pattern Recognition (CVPR)*, June 2016.
- [15] N. Chebrolu, T. Lbe, O. Vysotska, J. Behley, and C. Stachniss, "Adaptive robust kernels for non-linear least squares problems," *IEEE Robotics and Automation Letters*, vol. 6, no. 2, pp. 2240–2247, 2021.
- [16] P.-Y. Lajoie, S. Hu, G. Beltrame, and L. Carlone, "Modeling perceptual aliasing in SLAM via discretecontinuous graphical models," *IEEE Robotics and Automation Letters*, vol. 4, no. 2, pp. 1232–1239, 2019.
- [17] L. Carlone and G. C. Calafiore, "Convex relaxations for pose graph optimization with outliers," *IEEE Robotics and Automation Letters*, vol. 3, no. 2, pp. 1160–1167, 2018.
- [18] H. Yang, J. Shi, and L. Carlone, "TEASER: Fast and certifiable point cloud registration," *IEEE Transactions on Robotics*, vol. 37, no. 2, pp. 314–333, 2021.
- [19] E. M. Ronchetti and P. J. Huber, *Robust statistics*. John Wiley & Sons, 2009.
- [20] G. Agamennoni, P. Furgale, and R. Siegwart, "Self-tuning m-estimators," in *2015 IEEE International Conference on Robotics and Automation (ICRA)*, 2015, pp. 4628–4635.
- [21] A. Nakabayashi and G. Ueno, "Nonlinear filtering method using a switching error model for outlier-contaminated observations," *IEEE Transactions on Automatic Control*, vol. 65, no. 7, pp. 3150–3156, 2020.
- [22] H. Wang, H. Li, J. Fang, and H. Wang, "Robust Gaussian Kalman filter with outlier detection," *IEEE Signal Processing Letters*, vol. 25, no. 8, pp. 1236–1240, 2018.
- [23] A. H. Chughtai, M. Tahir, and M. Uppal, "Outlier-robust filtering for nonlinear systems with selective observations rejection," *IEEE Sensors Journal*, vol. 22, no. 7, pp. 6887–6897, 2022.
- [24] R. Pich, S. Srkk, and J. Hartikainen, "Recursive outlier-robust filtering and smoothing for nonlinear systems using the multivariate Student-t distribution," in *2012 IEEE International Workshop on Machine Learning for Signal Processing*, 2012, pp. 1–6.
- [25] M. A. Amaral Turkman, C. D. Paulino, and P. Miller, *Computational Bayesian Statistics: An Introduction*, ser. Institute of Mathematical Statistics Textbooks. Cambridge University Press, 2019.
- [26] S. Särkkä and L. Svensson, *Bayesian filtering and smoothing*. Cambridge university press, 2023, vol. 17.
- [27] V. Smídl and A. Quinn, *The variational Bayes method in signal processing*. Springer Science & Business Media, 2006.
- [28] K. P. Murphy, *Machine learning : a probabilistic perspective*. Cambridge, Mass. [u.a.]: MIT Press, 2013.
- [29] ———, "Conjugate Bayesian analysis of the Gaussian distribution," *def*, vol. 1, no. 2 σ 2, p. 16, 2007.
- [30] D. Fink, "A compendium of conjugate priors," See <http://www.people.cornell.edu/pages/df36/CONJINTRnew%20TEX.pdf>, vol. 46, 1997.
- [31] B. Curless and M. Levoy, "A volumetric method for building complex models from range images," in *Proceedings of the 23rd annual conference on Computer graphics and interactive techniques*, 1996, pp. 303–312.
- [32] Y. Xiang, R. Mottaghi, and S. Savarese, "Beyond PASCAL: A benchmark for 3D object detection in the wild," in *IEEE Winter Conference on Applications of Computer Vision*, 2014, pp. 75–82.
- [33] H. Yang and L. Carlone, "A polynomial-time solution for robust registration with extreme outlier rates," *Robotics: Science and Systems*, 2019.
- [34] F. Bai, T. Vidal-Calleja, and G. Grisetti, "Sparse pose graph optimization in cycle space," *IEEE Transactions on Robotics*, vol. 37, no. 5, pp. 1381–1400, 2021.